Dark Matter in SUGRA Models with Universal and Nonuniversal Gaugino Masses

D. P. Roy

Homi Bhabha Centre for Science Education

Tata Institute of Fundamental Research

Mumbai – 400088, India

Outline

- Nature of LSP in SUGRA Models: Bino, Higgsino or Wino
- DM Constraints on Bino & Higgsino LSP in mSUGRA Model
- Implications for Bino LSP Signals at LHC
- SUGRA Models with Nonuniversal Gaugino Masses

$$SU(5) \Rightarrow 24 \times 24 = 1(\tilde{B}) + 24(\tilde{B}) + 75(\tilde{H}) + 200(\tilde{H}) : gaugino - mass$$

- Bulk Annihilation Region of Bino LSP in 1+24, 1+75 & 1+200 Models : Implications for DM and LHC Expts.
- Mixed Bino-Higgsino & Bino-Wino-Higgsino LSP in 1+75 and 1+200 Models : Implications for DM and LHC Expts.
- Wino and Higgsino LSP in AMSB Model:Implications for DM

Nature of the Lightest Superparticle (LSP) in SUGRA Models:

Astrophysical Constraints ⇒ Colourless & Chargeless LSP
Direct DM Detection Expts ⇒ LSP not Sneutrino

$$\therefore LSP \rightarrow \chi \equiv \chi_1^0 = c_1\widetilde{B} + c_2\widetilde{W} + c_3\widetilde{H}_d + c_4\widetilde{H}_u$$

$$M_N = \begin{pmatrix} M_1 & 0 & -M_Z\sin\theta_W\cos\beta & M_Z\sin\theta_W\sin\beta \\ 0 & M_2 & M_Z\cos\theta_W\cos\beta & -M_Z\cos\theta_W\sin\beta \\ -M_Z\sin\theta_W\cos\beta & M_Z\cos\theta_W\cos\beta & 0 & -\mu \\ M_Z\sin\theta_W\sin\beta & -M_Z\cos\theta_W\sin\beta & -\mu & 0 \end{pmatrix}$$

Diagonal elements : M_1, M_2, ±μ in the basis $\widetilde{B}, \widetilde{W}$ & $\widetilde{H}_{1,2} = \widetilde{H}_d \pm \widetilde{H}_u$

Nondiagonal elements < M_Z

Exptl Indications ⇒ M_1, M_2, μ > $2M_Z$ in mSUGRA $\Rightarrow \chi \cong \widetilde{B}, \widetilde{W} or \widetilde{H}$

Exception : $M_{ii} \approx M_{jj} \Rightarrow \tan 2\theta_{ij} = 2M_{ij} / (M_{ii} - M_{jj})$ *large* $\Rightarrow \chi = \widetilde{B} - \widetilde{H}, \widetilde{W} - \widetilde{H}$

"Well-tempered Neutralino Scenario" Arkani-Hamed, Delgado & Giudice

DM Relic Density Constraints on Bino & Higgsino LSP Scenarios of

mSUGRA: SUSY Br in HS communicated to the OS via grav. Int.

$\Rightarrow$ m_0, $m_{1/2}$, $\tan\beta$, A_0, sign (μ) at GUT scale ($A0 = 0$ & +ve μ)

$\downarrow$ RGE (Weak Sc masses)

$$\widetilde{B} : M_1 = (\alpha_1 / \alpha_G) m_{1/2} \approx 0.4 m_{1/2} \;\&\; \widetilde{W} : M_2 = (\alpha_2 / \alpha_G) m_{1/2} \approx 0.8 m_{1/2}$$

Imp Weak Sc Scalar mass M_{Hu}

$$EWSB \Rightarrow \mu^2 + M_Z^2 / 2 = \frac{M_{Hd}^2 - M_{Hu}^2 \tan^2\beta}{\tan^2\beta - 1} \approx -M_{Hu}^2 \,@\, \tan\beta > 5$$

(LEP)

$$||$$

RGE: $$-M_{Hu}^2 = \underbrace{C_1}_{-\varepsilon}(\alpha_i, h_t, \tan\beta) m_0^2 + \underbrace{C_2}_{\approx 2}(\alpha_i, h_t, \tan\beta) m_{1/2}^2$$

Hyperbolic Br (tan $\beta > 5$) of μ^2:

$$m_0 \approx m_{1/2} \Rightarrow |\mu| > M_1 \Rightarrow \tilde{B} : LSP$$

$$m_0 >> m_{1/2} \Rightarrow |\mu| \leq M_1 \Rightarrow \tilde{B} - \tilde{H} : Mixed - LSP .or. \tilde{H} : LSP$$

Chattopadhyay et al

$m_0 \sim m_{1/2} \rightarrow$ TeV (Bino LSP)

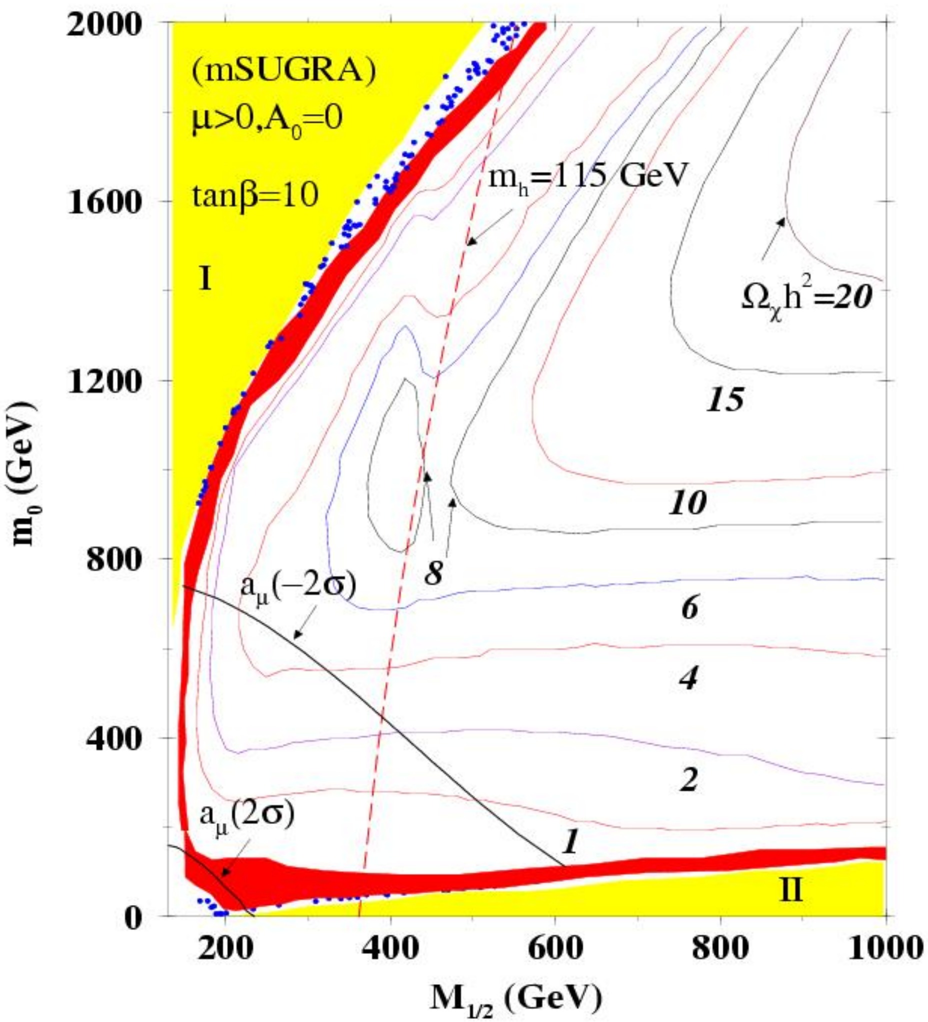

$m_h > 115$ GeV $\Rightarrow m_{1/2} > 400$ GeV ($M_1 > 2M_Z$)
$\Rightarrow$ also large sfermion mass

Bino does not carry any gauge charge
$\Rightarrow$ Pair annihilate via sfermion exch

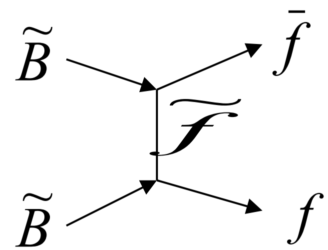

Large sfermion mass $\Rightarrow$ too large Ωh^2
Except for the stau co-ann. region

$m_{\tilde{\tau}} \cong m_{\tilde{B}}$

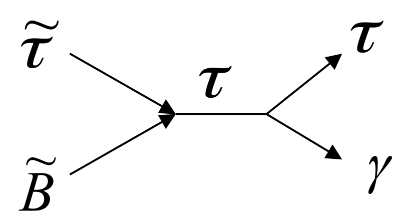

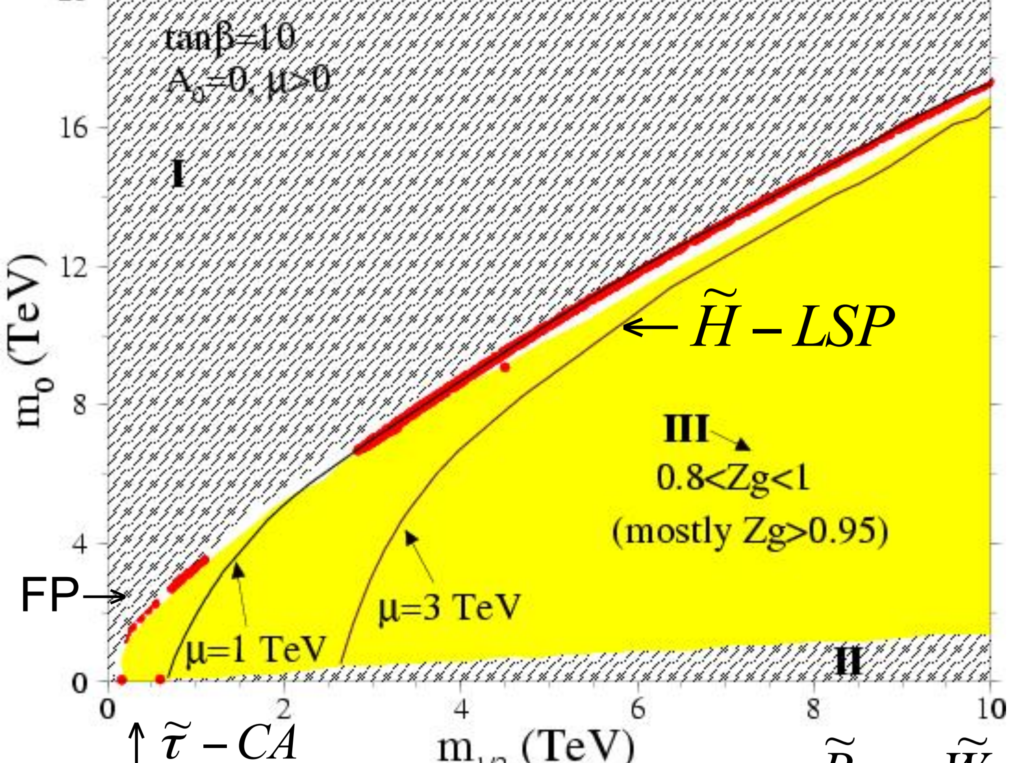

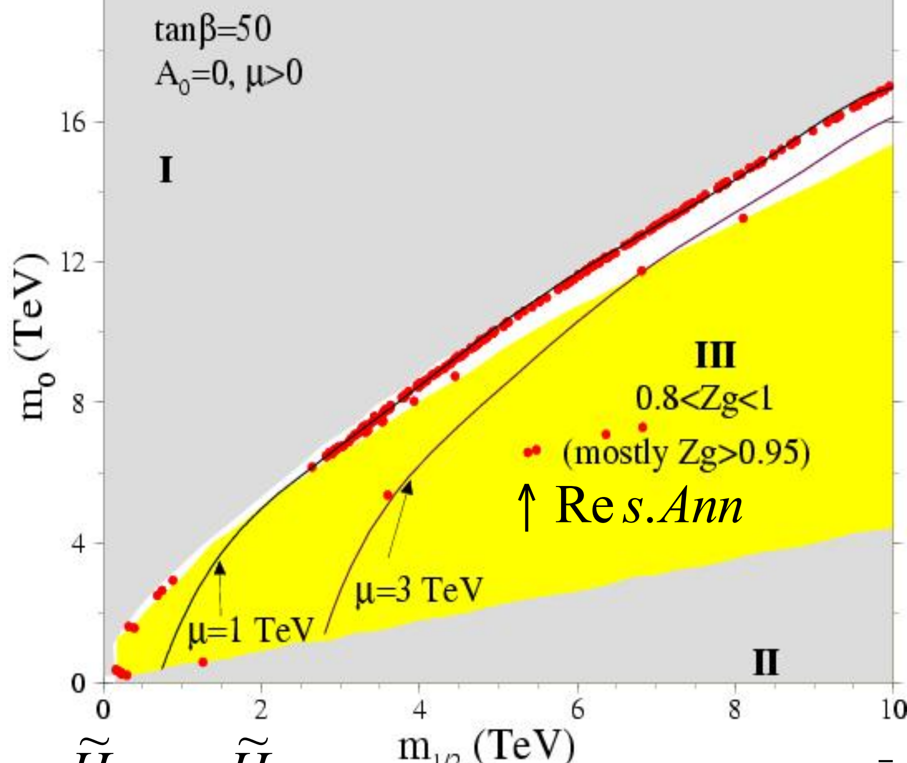

$$\chi = c_1\widetilde{B} + c_2\widetilde{W} + c_3\widetilde{H}_d + c_4\widetilde{H}_u$$

$$\widetilde{\tau} - CoAnn : m_{\widetilde{\tau}} \cong M_1 (within \approx 10\%) \quad \mathrm{Re}\,s.Ann : M_A \cong 2M_1$$

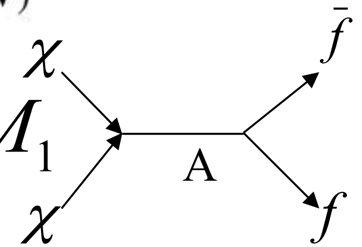

$$Focus - Pt : \mu \cong M_1 (\chi = \widetilde{B} - \widetilde{H})$$

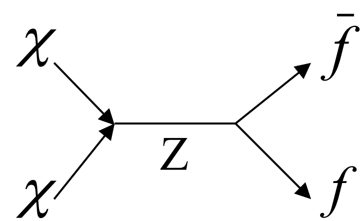

$$g_{Z\chi\chi} \propto c_3^2 - c_4^2$$

$$\widetilde{H} - LSP : M_{\widetilde{H}^{\pm,0}} \cong \mu \cong 1TeV$$

$$g_{A\chi\chi}, g_{H\chi\chi} \propto c_{1,2}c_{3,4}$$

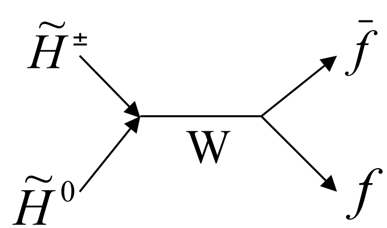

$$(m_\phi \approx m_0 > 7TeV)$$

Bino LSP Signal at LHC :

$$\tilde{q}\bar{\tilde{q}} \rightarrow q\bar{q}\chi\chi \rightarrow jj \not{E}_T ; \tilde{g}\tilde{g} \rightarrow q\bar{q}q\bar{q}\chi\chi \rightarrow jjjj \not{E}_T$$

Canonical Multijet + Missing-E_T signal with possibly additional jets (leptons) from cascade decay (Valid through out the Bino LSP parameter space, including the **Res.Ann Region**)

Focus Point Region: $M_{Hu}^2 = m_0^2 - (3/2)\underbrace{y_t}_{\approx 2/3} m_0^2 - \underbrace{C_2}_{\approx 2} m_{1/2}^2 = +\varepsilon m_0^2 - 2m_{1/2}^2 = -\mu^2 - M_Z^2/2$

$$m_0 >> m_{1/2} \Rightarrow small|\mu| \approx M_1$$

Inverted Hierarchy

$$m_{\tilde{t}_1}^2 = m_0^2 - \underbrace{y_t}_{2/3} m_0^2 + Cm_{1/2}^2 = (1/3)m_0^2 + Cm_{1/2}^2 ; m_{\tilde{u},\tilde{d}}^2 = m_0^2 + Cm_{1/2}^2$$

$$m_0 = 2TeV, m_{1/2} = 0.5TeV \ \& \tan\beta = 10$$

$$\Rightarrow m_{\tilde{g}} = 1.3TeV, m_{\tilde{t}_1} = 1.5TeV, m_{\tilde{u},\tilde{d}} \geq 2.2TeV$$

$$\Rightarrow \tilde{g} \xrightarrow{\tilde{t}_1} \bar{t}t\chi_i^0, \bar{t}b\chi_j^+ \rightarrow 2b2W\chi...$$

$$\Rightarrow \tilde{g}\tilde{g} \rightarrow 4b + 4W(\rightarrow leptons) + \not{E}_T$$

SUSY Signal at LHC: Focus Pt. Region

$$4b + jets + \not{E}_T + (1-4)l$$

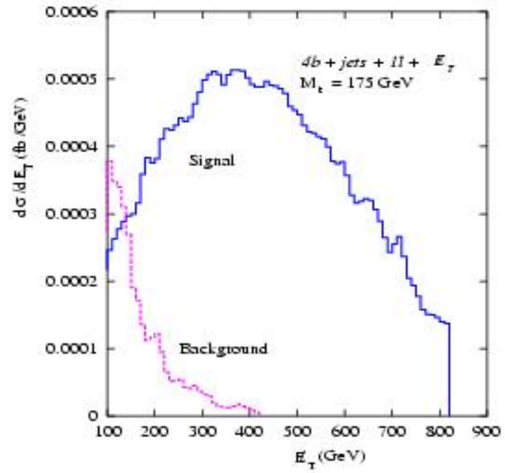

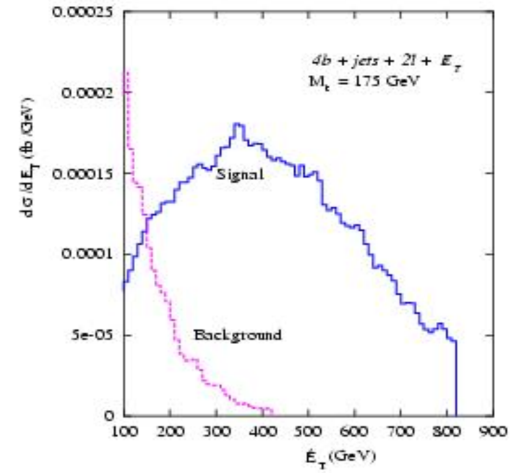

Chattopadhyay et al, PLB 2000

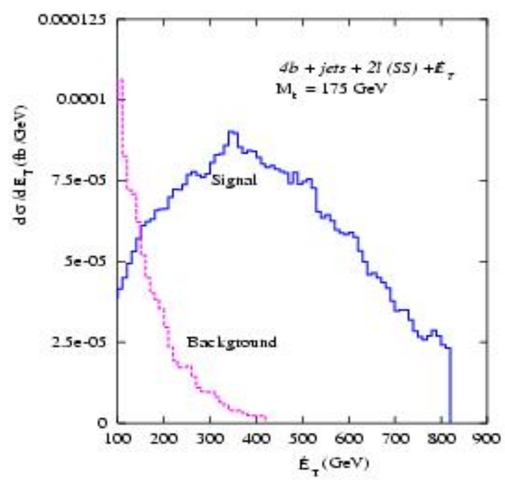

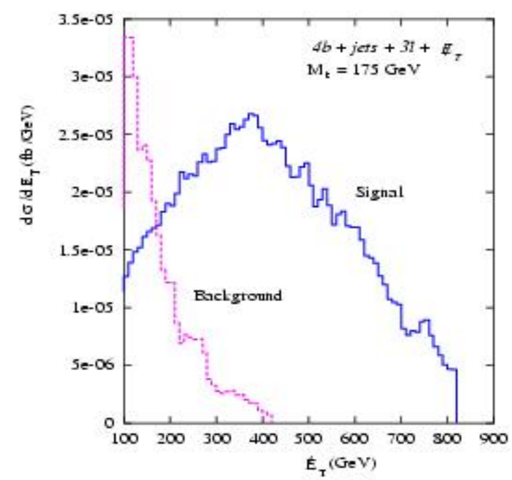

$\tilde{\tau}$ Co-annihilation region

Guchait & Roy, PLB '02

$$m_{\tilde{\tau}_1} \cong m_\chi$$

$$\chi_1^\pm \to \nu\tilde{\tau}_1, \tilde{\tau}_1 \to \chi\tau$$

BR ≈ 1　　BR = 1

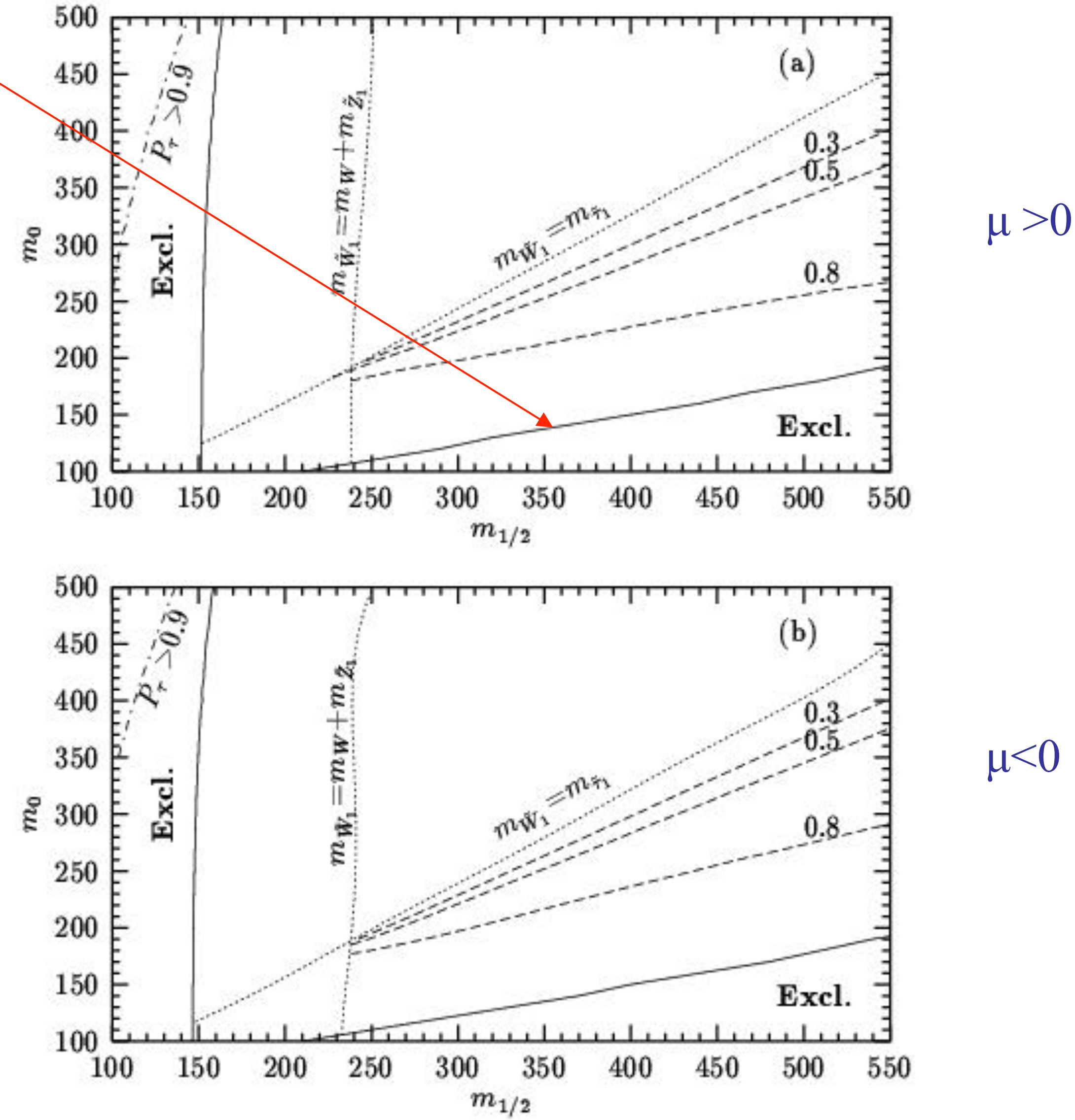

$$\tilde{W}_1 \equiv \chi_1^\pm, \tilde{Z}_1 \equiv \chi$$

τ is soft, but $P_\tau \approx +1$

One can use P_τ to detect the Soft τ coming from

$$\tilde{\tau}_1 \to \chi\tau.$$

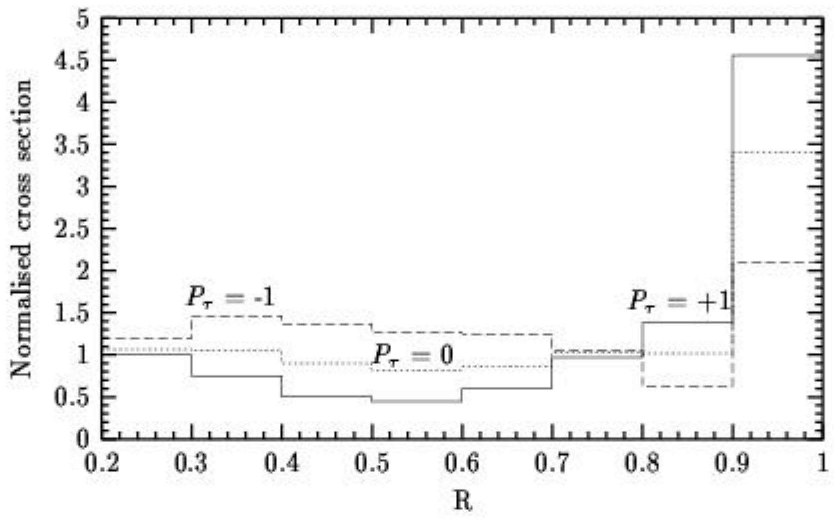

$$R = \frac{p_{\pi^\pm}}{p_{\tau-jet}}$$

$\tau^\pm \to \nu \underbrace{\pi^\pm \pi^0 s}_{\tau-jet}$: 1-prong hadronic τ decay (BR≈0.5)

With p_T > 20 GeV cut for the τ-jet the τ misid. Probability from QCD jets goes down from 6% for R > 0.3 ($p_{T\pi\pm}$> 6 GeV) to 0.25% for R > 0.8 ($p_{T\pi\pm}$ > 16 GeV), while retaining most Of the signal.

Soft τ signal from $\tilde{\tau}_1 \rightarrow \tau\chi$ decay in the co-annihilation region $\left(m_{\tilde{\tau}_1} \cong m_{\chi}\right)$

Godbole, Guchait and Roy, PRD '09

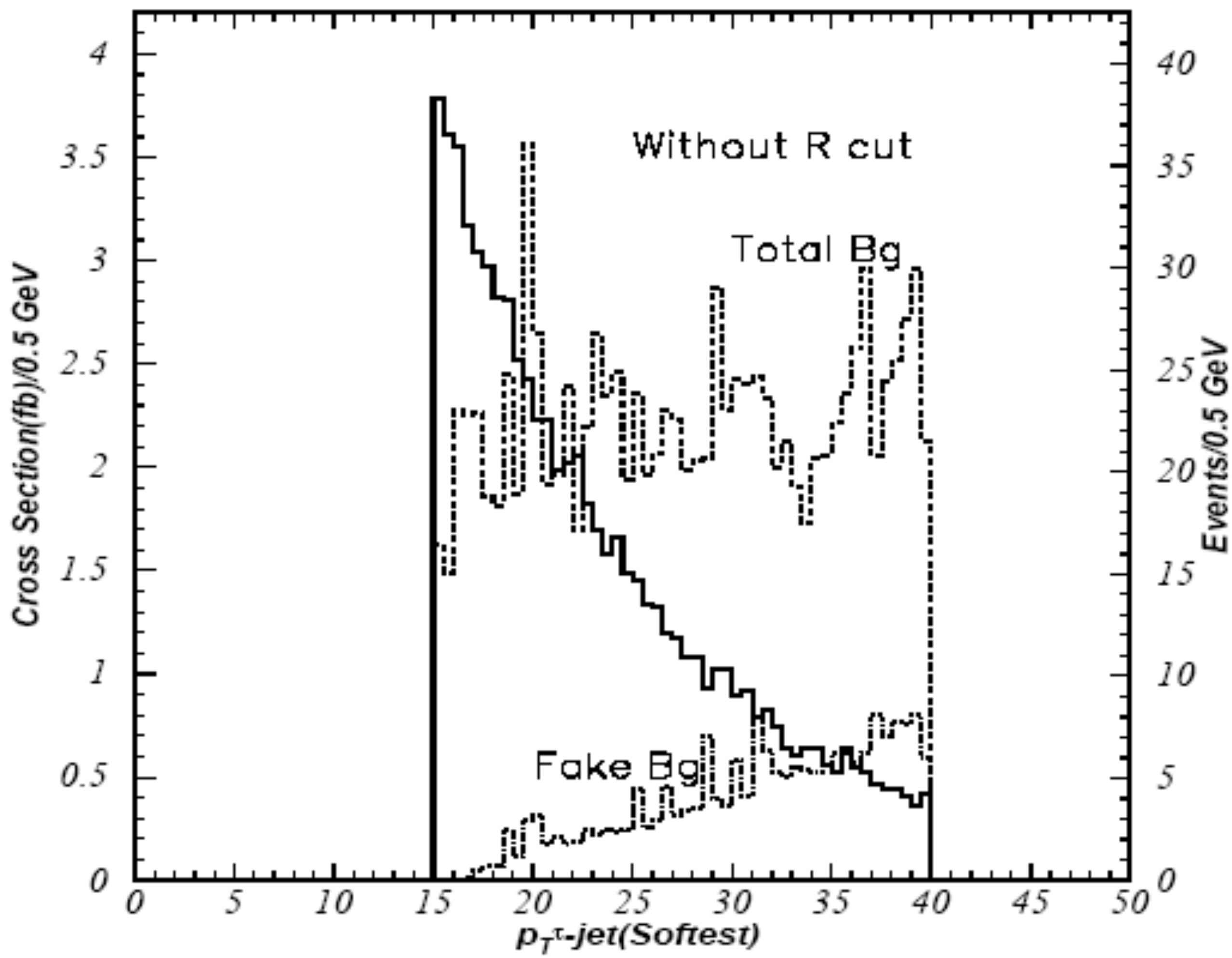

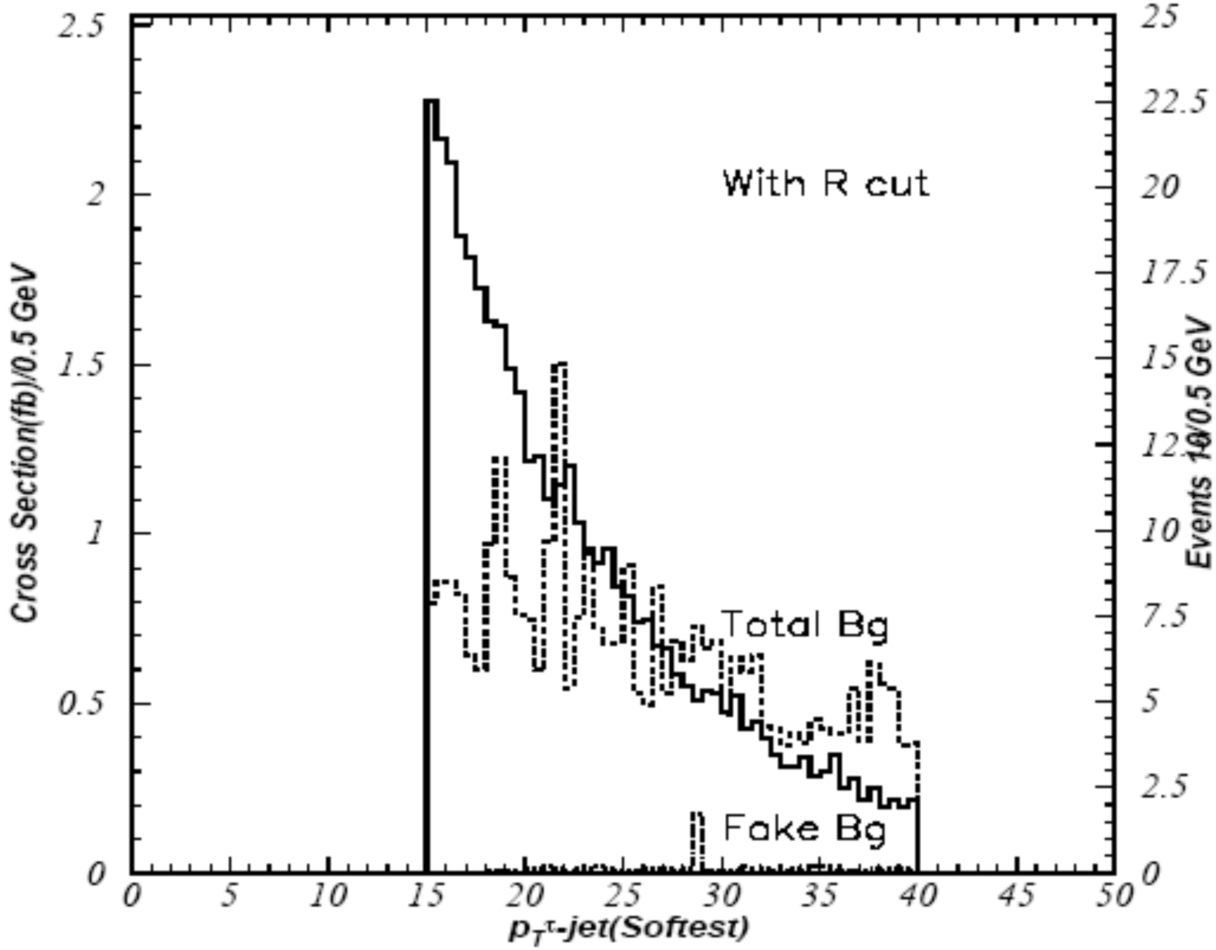

Figure 2: Same as Fig.1, but with R cut of eq.(8).

N(15-25 GeV)/N(25-40 GeV) = 2.3 for Signal and 1.0 for BG.

So the steep rise of the Signal at the low PT end can be used to distinguish it from the BG and also to measure the small mass difference $\Delta m = m_{\tilde{\tau}_1} - m_{\chi} \simeq 10 GeV$.

Nonuniversal gaugino mass models of SUGRA

n	M_3^G	M_2^G	M_1^G
1	1	1	1
24	1	$-3/2$	$-1/2$
75	1	3	-5
200	1	2	10

$$M_i^G \equiv M_{\lambda i} \in \frac{\langle F_S \rangle_{ij}}{M_{Pl}} \lambda_i \lambda_j ; i \,\&\, j = 1,2,3$$

$$SU(5) : F_S \supset 24 \otimes 24 = 1 + 24 + 75 + 200$$

$$F_S = 1 \Rightarrow M_{1,2,3}^G = m_{1/2} (Universal) \Rightarrow M_1 \cong 0.4 m_{1/2} < \mu \cong \sqrt{2} m_{1/2} : \tilde{B} - LSP$$

$$F_S = 24 \Rightarrow M_{1,2,3}^G = (-1/2, -3/2, 1) \times m_{1/2} \Rightarrow |M_1| \cong 0.2 m_{1/2} < \mu : \tilde{B} - LSP$$

$$F_S = 75 \Rightarrow M_{1,2,3}^G = (-5, 3, 1) \times m_{1/2} \Rightarrow |M_1| \cong 2 m_{1/2} > \mu \Rightarrow \tilde{H} - LSP$$

$$F_S = 200 \Rightarrow M_{1,2,3}^G = (10, 2, 1) \times m_{1/2} \Rightarrow M_1 \cong 4 m_{1/2} > \mu \Rightarrow \tilde{H} - LSP$$

$$\mu^2 + M_Z^2 / 2 \cong -0.1 m_0^2 + 2.1 M_3^{G2} - 0.2 M_2^{G2} + 0.2 M_3^G M_2^G$$

Chattopadhyay & Roy, Huitu et al, Anderson et al, …

$$\langle F_S \rangle = (1-\kappa) \langle F_1 \rangle + \kappa \langle F_{24,75,200} \rangle$$

M3 = 300, 400, 500 & 600 GeV

Bino LSP in Non-universal Gaugino Mass Model

King, Roberts & Roy, JHEP 07

Bulk annihilation region of Bino DM (yellow) allowed in Non-universal gaugino mass models

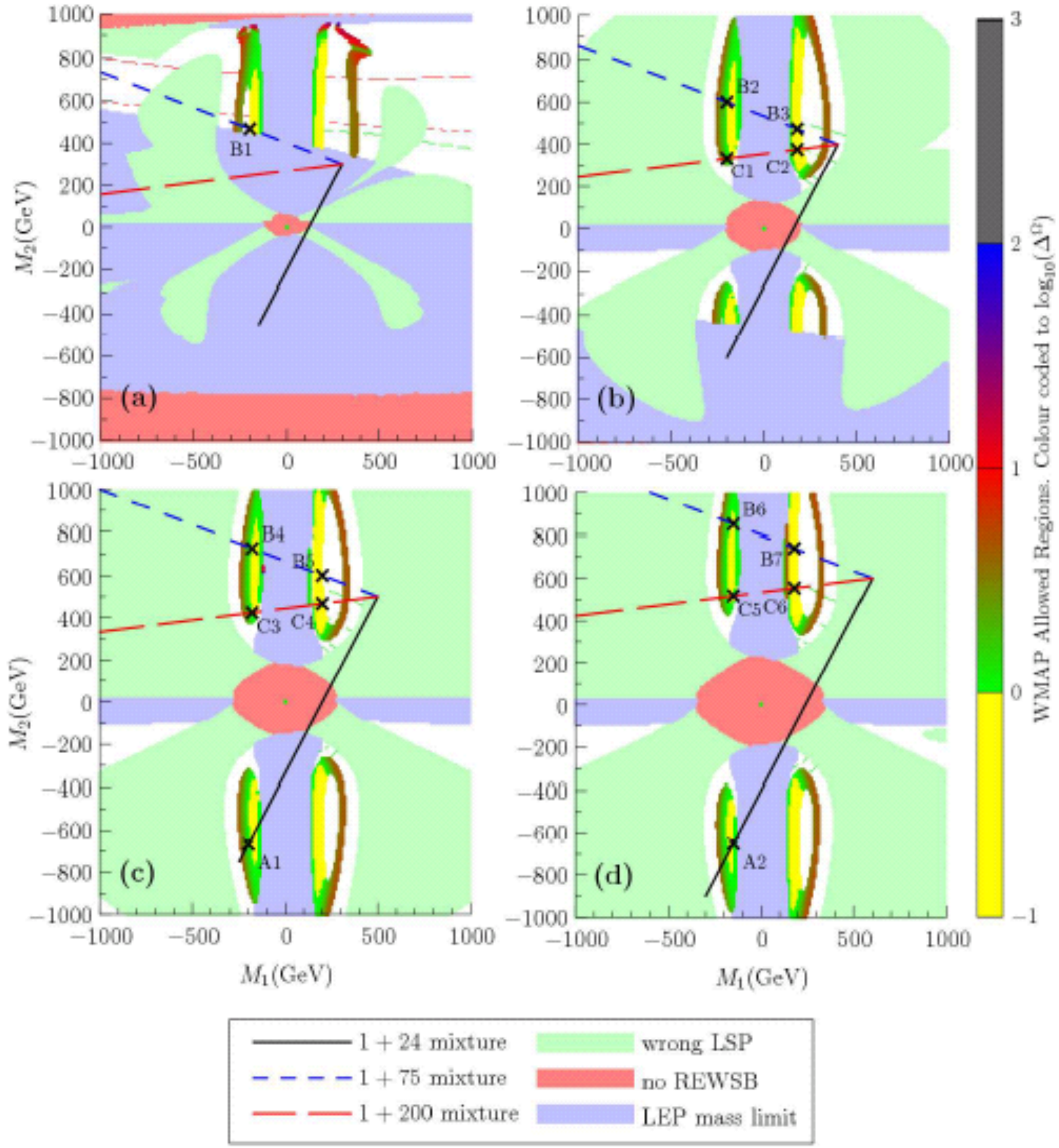

Light right sleptons
Even left sleptons lighter than Wino
=>Large leptonic BR of SUSY
Cascade decay via Wino at LHC

$$\chi_1^0 + \chi_1^0 \xrightarrow{\tilde{e}} e^+ + e^- + \gamma$$

Hard Positron Signal (PAMELA?)

Particle	Mass (GeV)
$\tilde{\chi}_1^0$ (bino)	78.1
$\tilde{\chi}_2^0$ (wino)	457
$\tilde{\chi}_3^0$ (higgsino)	614
$\tilde{\chi}_4^0$ (higgsino)	636
$\tilde{\chi}_1^+$ (wino)	461
$\tilde{\chi}_2^+$ (higgsino)	635
M_1	81
M_2	470
μ	611
$\tilde{g}$	1150
$\tilde{\tau}_1$	104
$\tilde{\tau}_2$	399
$\tilde{e}_R, \tilde{\mu}_R$	115
$\tilde{e}_L, \tilde{\mu}_L$	399
$\tilde{t}_1$	793
$\tilde{t}_2$	1025
$\tilde{b}_1$	980
$\tilde{b}_2$	1000
$\tilde{q}_{1,2,R}$	$\sim$ 1005
$\tilde{q}_{1,2,L}$	$\sim$ 1070

Mixed bino-higgsino LSP (DM)
1+75 Model
Chattopadhyay, Das & Roy, PRD 09

$$m_{1/2} = (1-\kappa)m_{1/2}^{1} + \kappa m_{1/2}^{75}; \kappa = 0.475$$

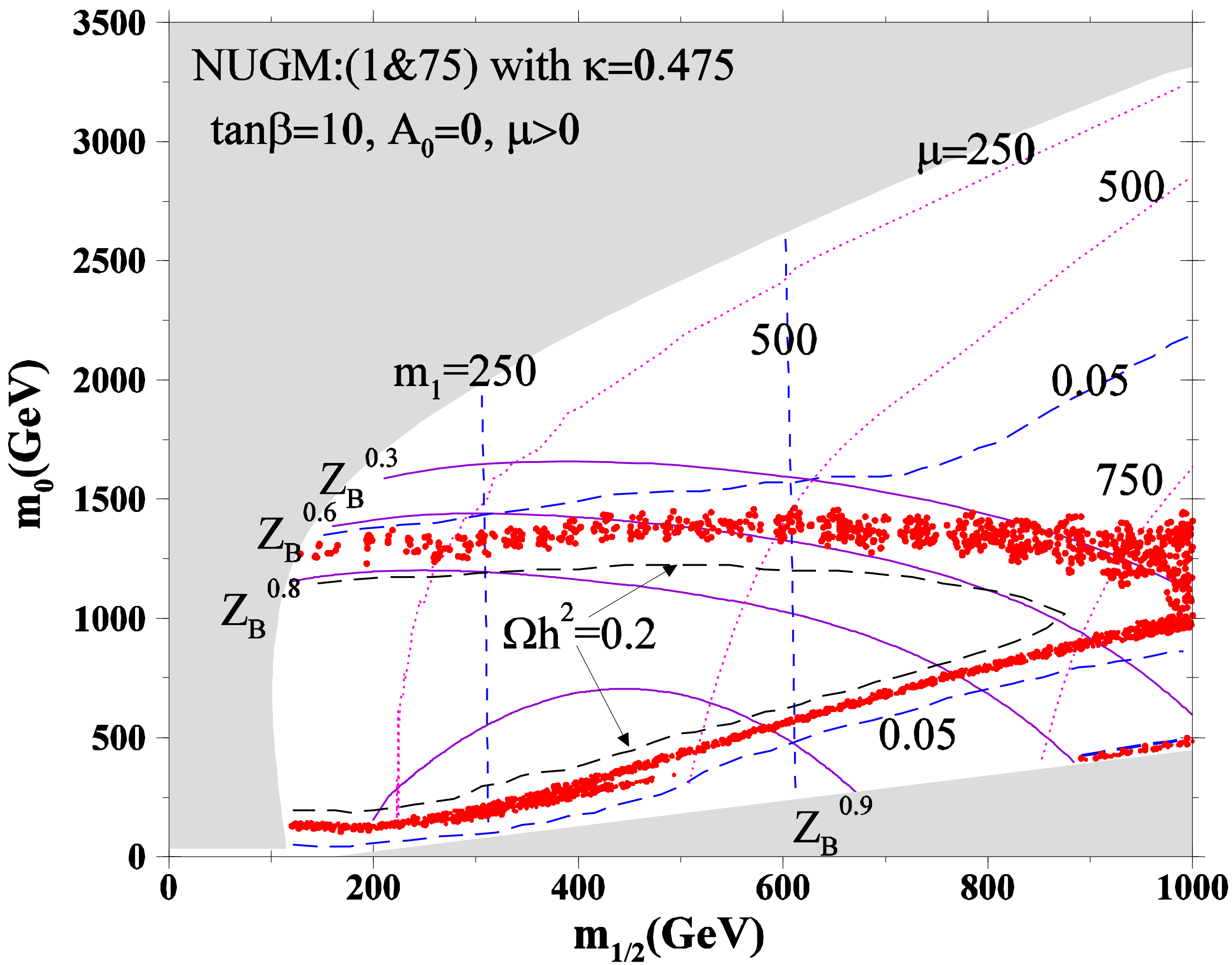

$$1 + 200 Model \Rightarrow m_{1/2} = (1-\kappa) m_{1/2}^{1} + \kappa m_{1/2}^{200}; \kappa = 0.12$$

Mixed bino-wino-higgsino LSP (DM)

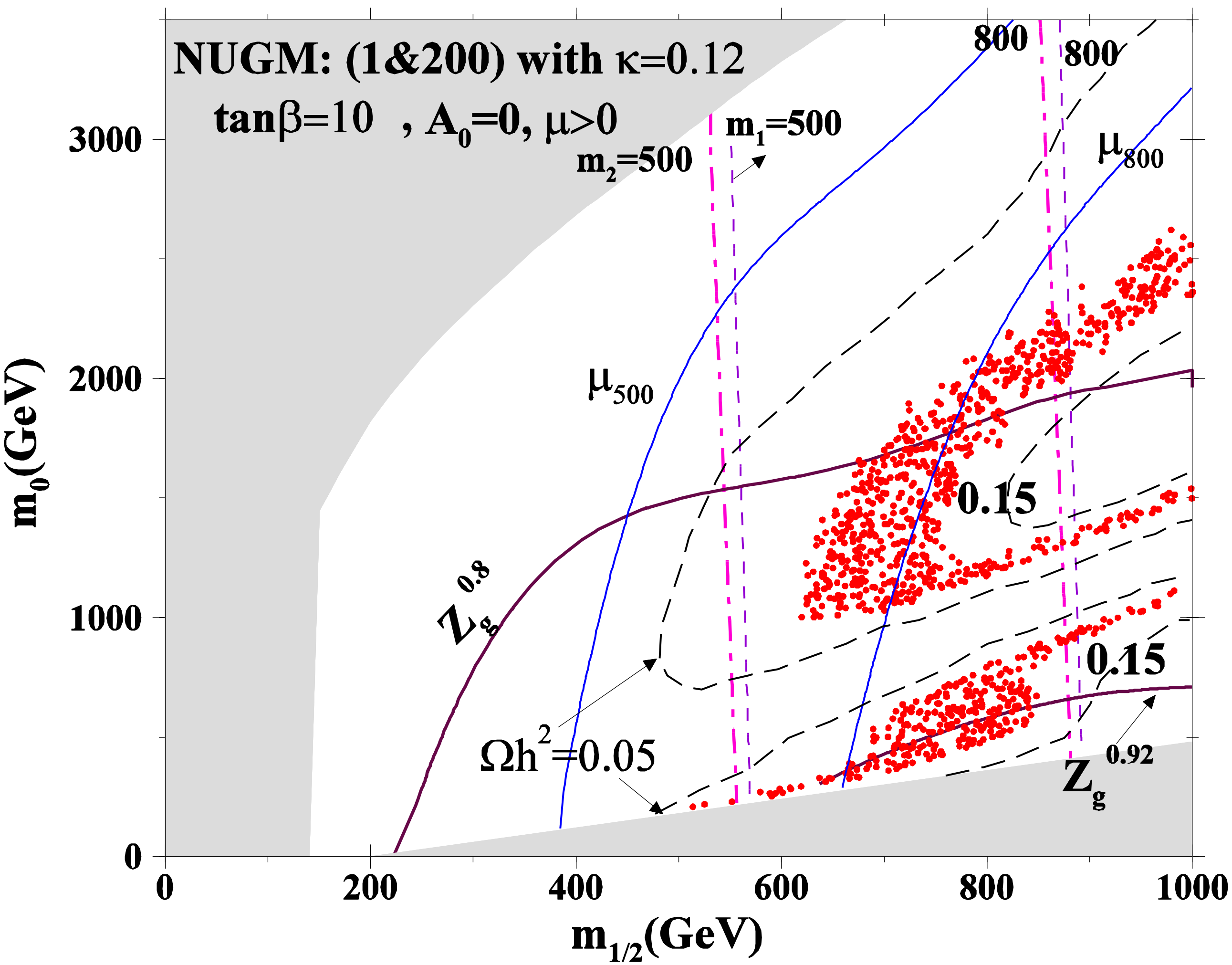

Bino, Higgsino & Wino LSP Signals in Dark Matter Detection Expts

1. Direct Detection (CDMS, XENON,…)

$$\chi = c_1\tilde{B} + c_2\tilde{W} + c_3\tilde{H}_d + c_4\tilde{H}_u$$

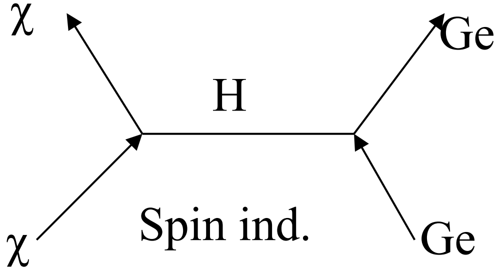

$$g_{Z\chi\chi} \propto c_3^2 - c_4^2 \;\&\; g_{H\chi\chi} \propto c_{1,2}c_{3,4}$$

Best for mixed DM $\rightarrow \;\; \chi \simeq \tilde{B}/\tilde{W} - \tilde{H}$

Not for pure bino, wino or higgsino DM

2. Indirect Detection via HE ν from χχ annihilation in the Sun (Ice Cube,Antares)

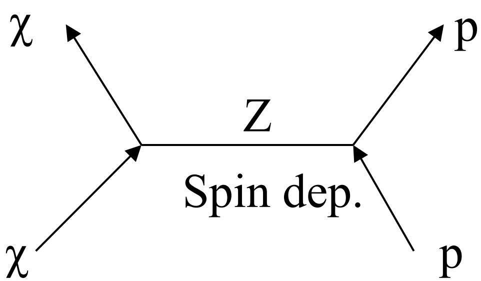

$$R_{\chi\chi}^{ann.} = R_{\chi}^{trap} \propto \sigma_{\chi p} \propto g_{Z\chi\chi}^2 \propto (c_3^2 - c_4^2)^2$$

$$\Rightarrow OK.\,for\,\chi = mixed(\tilde{B} - \tilde{H})$$

$$\Rightarrow Not.\,for\,\chi \cong \tilde{B}, \tilde{W} \;\&\; \tilde{H} \equiv \tilde{H}_d \pm \tilde{H}_u$$

Roy, PRD ‘10
($\alpha_{75} \equiv \kappa$)

Fig 1. Prediction of the (1+75) model compared with the putative signal corridor of the two candidate events of the CDMS II expt. The blue dots denote the WMAP DM relic density compatible points.

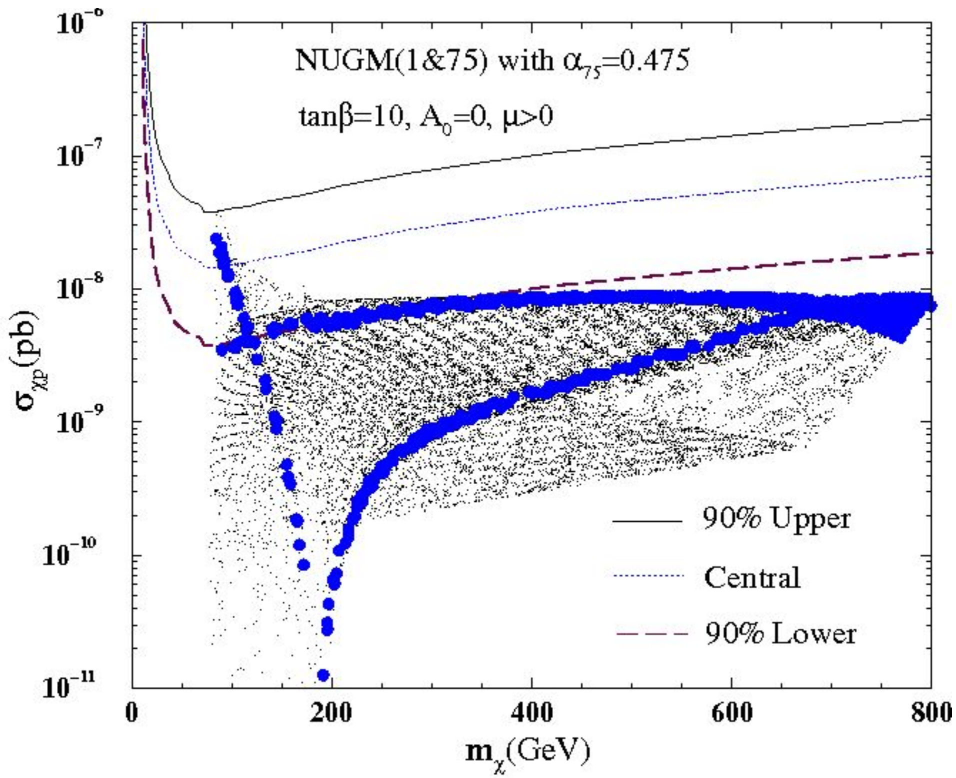

Table 1. Superparticle masses (in GeV) for a WMAP compatible point in the intersection region of the (1 + 75) model prediction with the CDMS II candidate events of Fig 1, corresponding to $m_{1/2}$ = 144 GeV and m_0 = 1255 GeV. All the remaining sfermion and Higgs boson masses are around 1250 GeV.

$\chi^0_1(\chi)$	χ^0_2	χ^0_3	χ^0_4	$\chi^\pm_1$	$\chi^\pm_2$	$\tilde{g}$	$\tilde{t}_1$	$\tilde{t}_2$	$\tilde{b}_1$	h^0
103	120	168	270	121	270	433	760	1063	1054	112

Low gluino mass (≤ 800 GeV) => Viable LHC Signal at 7 TeV.

Fig 2. Prediction (1+200) model prediction with the putative signal corridor, corresponding to the two candidate events of the CDMS II expt. Blue dots correspond to the points, compatible with the WMAP DM relic density.

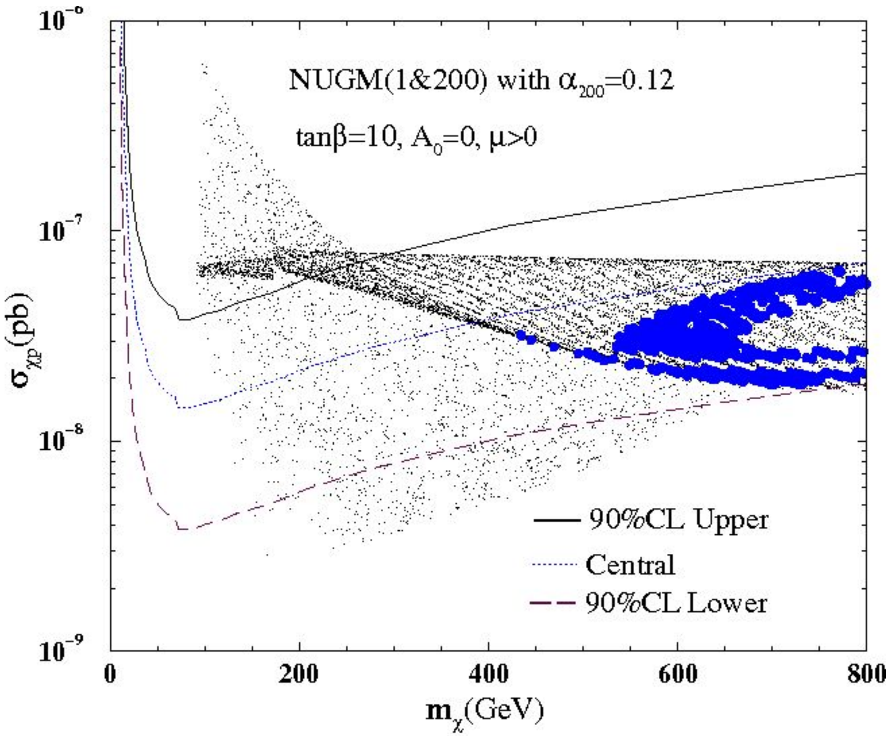

$m_{1/2}$	m_0	$\chi^0_1(\chi)$	χ^0_2	χ^0_3	χ^0_4	χ^+_1	χ^+_2	$\tilde{g}$	$\tilde{t}_1$	$\tilde{t}_2$	$\tilde{b}_1$	h^0
725	1450	633	657	794	822	643	818	1700	1460	1813	1801	117
900	1357	798	818	985	1009	807	1005	2045	1649	2013	2001	118

(Other squark masses are in the 2000-2200 GeV range)

Inverted Hierarchy => Decay of the gluino pair via stop

⇒3-4 top quarks in addition to the missing- E_T (like the focus pt. region)

⇒Multiple isolated leptons and b-tags + missing-E_T .

⇒Gluino mass of 2.0-2.5 TeV requires LHC run at 14TeV

PROBING A MIXED NEUTRALINO DARK MATTER MODEL

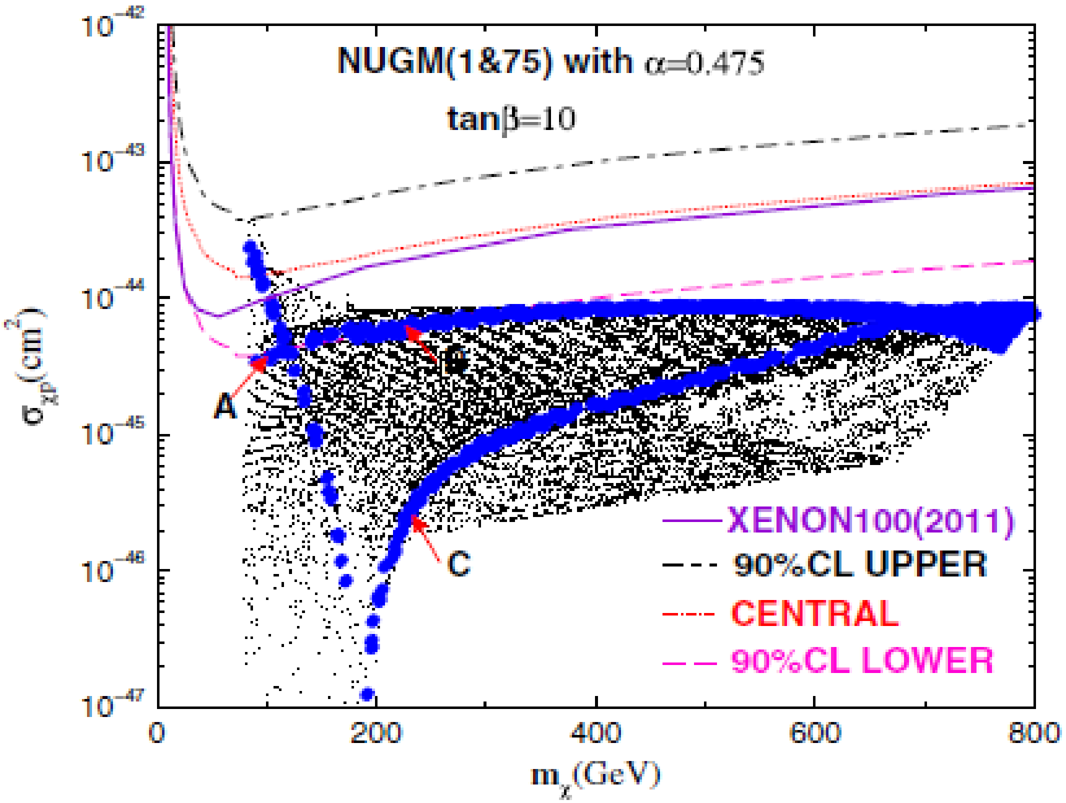

Guchait, Sengupta & DPR
PRD 85, 035024 (2012)

TABLE I. Mass spectrum (in GeV) for the three representative parameter points (A) $m_{1/2} = 144$ GeV, $m_0 = 1255$ GeV, (B) $m_{1/2} = 300$ GeV, $m_0 = 1325$ GeV, (C) $m_{1/2} = 300$ GeV, $m_0 = 185$ GeV. For all cases $\tan\beta = 10$ and $A_0 = 0$.

Model	$\tilde{g}$	$\tilde{q}_L$	$\tilde{q}_R$	$\tilde{t}_1$	$\tilde{b}_1$	$\tilde{e}_l$	$\tilde{\tau}_1$	χ_1^0	χ_2^0	χ_1^+	χ_2^+
A	433	1280	1274	759	1054	1263	1246	104	122	123	271
B	793	1480	1440	902	1246	1375	1327	227	256	257	501
C	722	750	660	483	649	437	237	231	301	302	490

TABLE II. Decay branching ratios of sparticles for three representative points A, B, and C, as shown in Table I.

Decays	A	B	C
$\tilde{g} \to \tilde{q}q$			43%
$\tilde{g} \to \tilde{b}b$			17%
$\tilde{g} \to \tilde{t}t$			40%
$\tilde{t}_1 \to b\chi_1^{\pm}$			88%
$\tilde{q}_L \to q\chi_{1,2}^{\pm}$			62%
$\tilde{q}_L \to q\chi_{1,2,3,4}^{0}$			32%
$\tilde{g} \to t\bar{b}\chi_1^{\pm}$	25%	54%	
$\tilde{g} \to g\chi_{2,3}^{0}$	30%	4.2%	
$\tilde{g} \to q\bar{q}\chi_{1,2}^{\pm}$	16%	2.6%	
$\tilde{g} \to b\bar{b}\chi_{1,2,3,4}^{0}$	12%	2%	
$\tilde{g} \to t\bar{t}\chi_{1,2,3,4}^{0}$		27%	
$\tilde{g} \to q\bar{q}\chi_{1,2,3,4}^{0}$	17%	2%	
$\chi_1^{+} \to q\bar{q}\chi_1^{0}$	68%	67%	
$\chi_1^{+} \to e\bar{e}\chi_1^{0}$	22%	22%	
$\chi_1^{+} \to \tilde{\tau}\nu_{\tau}$			100%
$\chi_2^{0} \to q\bar{q}\chi_1^{0}$	68%	66%	
$\chi_2^{0} \to \tilde{\tau}_1\tau$			84%
$\chi_2^{0} \to \tilde{e}e$			16%

TABLE III. The signal and SM background events for dilepton final states. The $t\bar{t}$ and QCD backgrounds events are simulated for different $\hat{p}_T$ bins as shown. In the case of $t\bar{t}$ background, we multiply cross sections by the K factor 1.6 to take into account next-to-leading order effects [20]. (Energy units are in GeV.)

Proc	Cross section (pb)	N_{ev}	2ℓ & $n_j \geq 3$	$\not{E}_T \geq 100$	Meff ≥ 500	$R_{ll} \leq 0.25$	SS, OS	$m_{\ell\ell} \neq 75$–110	1 fb^{-1} SS OS	5 fb^{-1} SS OS
A: $\tilde{g}\,\tilde{g}$	5.84	10 k	185	134	75	61	16,45	16,36	10.0,21.0	50.,105
A: $\tilde{q}\,\tilde{g}$	0.28	10 k	342	303	301	279	89 190	89 150	2.5, 4.2	12.5,23
Total									12.5,25.2	62.5126.0
B: $\tilde{g}\,\tilde{g}$	0.06	10 k	737	609	503	382	142 240	142 198	1.0,1.2	5,6.0
B: $\tilde{q}\,\tilde{g}$	0.018	10 k	492	359	317	290	12 188	12 111	0,.2	0.,1.0
Total									1.0, 1.4	5.,7.0
C: $\tilde{g}\,\tilde{g}$	0.1	10 k	401	351	306	233	41 192	41 135	0.4,1.5	2.0,7.5
C: $\tilde{q}\,\tilde{g}$	0.57	10 k	492	359	317	290	12 188	12 111	0.75,6.3	3.75,31.5
C: $\tilde{q}\,\tilde{q}$	0.55	10 k	395	348	333	234	13 221	13 145	0.8,8	4,40
Total									1.96,15.8	9.8,79
$t\bar{t}$										
5–200	143.5	100 k	227	78	31	13	2,11	2,9	3,13.0	15,65
200–500	16.3	50 k	292	145	87	33	5,28	5,22	1.6, 7.1	8,35.5
500-inf	0.16	10 k	87	65	63	26	6,20	6,19	0.09,0.3	0.45, 1.5
Total									4.69,20.4	23.45 102
QCD										
200–300	6983	1 M	1	1	0	0	0,0	0,0	0,0	0,0
300–500	873	1 M	15	2	2	1	1,0	1,0	0.9,0	4.5,0
500–800	43.1	100 k	4	2	2	0	0,0	0,0	0,0	0,0
Total									0.9,0.0	4.5,0.

TABLE IV. The signal and background events, same as Table III, but for single lepton final states. The last two columns show the number of events multiplied by proper b-tagging efficiency for two luminosity options.

Proc	Cross section (pb)	N	Single lep.	$n_j \geq 4$	$m_T \geq 70$	$\not{E}_T \geq 150$	$M_{\rm eff} \geq 500$	$R_l \leq 0.1$	$n_b \geq 3$	1 fb^{-1}	5 fb^{-1}
A: $\tilde{g}\,\tilde{g}$	5.84	10 k	2270	570	308	143	98	42	7	1.25	6.25
A: $\tilde{q}\,\tilde{g}$	0.28	10 k	1440	1222	684	523	519	387	56	0.6	3.0
A: Total										1.85	9.25
B: $\tilde{g}\,\tilde{g}$	0.06	10 k	1987	1703	1208	865	789	440	136	0.4	2.0
B: $\tilde{q}\,\tilde{g}$	0.018	10 k	2702	1867	1348	1153	1150	889	268	0.023	0.12
B: Total										0.42	2.12
C: $\tilde{g}\,\tilde{g}$	0.1	10 k	1334	909	683	513	466	258	68	0.2	1.0
C: $\tilde{q}\,\tilde{g}$	0.57	10 k	1057	957	459	330	301	214	12	0.2	1.0
C: $\tilde{q}\,\tilde{q}$	0.55	10 k	882	266	198	139	135	59	2	<1	<1
C: Total										0.4	2.0
$t\bar{t}$											
5–200	143.52	100 k	23255	1296	607	78	36	5	0	0	
200–500	16.32	50 k	11196	2044	952	382	267	41	2	0.27	1.35
500–inf	0.16	10 k	2030	458	233	152	151	32	5	0.02	0.1
Total										0.29	1.45
QCD											
200–300	6896	1 M	12413	0	0	0	0	0	0	0	
300–500	873	1 M	1274	252	13	0	0	0	0	0	
500–800	43.1	100 k	158	39	2	1	0	0	0	0	
QCD: Total											

TABLE V. The signal and background events after, same as Table III, but for jets + $\not{E}_T$ final states. The kinematic selection cuts are described in the text. The last two columns present the number of events with respective luminosities as shown.

Proc	Cross section (pb)	N	$T \leq 0.95$	$R_T \leq .9$	$\not{E}_T \geq 200$	$H_T \geq 500$	$n_b \geq 3$	1 fb^{-1}	5 fb^{-1}
A: $\tilde{g}\,\tilde{g}$	5.84	10 k	6900	3170	446	301	32	6.6	33.0
A: $\tilde{q}\,\tilde{g}$	0.28	10 k	8332	4356	2042	2002	315	3.4	17.0
Total								10	50
B: $\tilde{g}\,\tilde{g}$	0.06	10 k	8708	5901	2901	2584	779	2.07	10.35
B: $\tilde{q}\,\tilde{g}$	0.018	10 k	9100	6263	4212	4177	1322	1.02	5.1
Total								3.09	15.45
C: $\tilde{g}\,\tilde{g}$	0.1	10 k	7623	3700	2888	1761	404	1.13	5.65
C: $\tilde{q}\,\tilde{g}$	0.57	10 k	5933	1984	1145	1030	121	1.82	9.1
C: $\tilde{q}\,\tilde{q}$	0.55	10 k	3326	729	433	385	17	0.3	1.5
Total								3.25	16.25
$t\bar{t}$									
5–200	143.5	100 k	37162	14548	21	14	0	0	0
200–500	16.32	50 k	27831	8559	109	54	3	0.48	2.4
500–inf	0.16	10 k	1741	482	68	64	7	0.09	0.45
Total								0.57	2.85
QCD									
300–500	873	1 M	194636	27532	7	5	0	0	0
500–800	43.1	100 k	19100	2329	9	9	0	0	0
200–300	6983	1 M	123	14	0	0	0	0	0

Wino LSP (mAMSB model)

SUSY braking in HS in communicated to the OS via the Super-Weyl Anomaly Cont. (Loop)

$$M_\lambda = \frac{\beta_g}{g} m_{3/2} \Rightarrow M_1 = \frac{33}{5}\frac{g_1^2}{16\pi^2} m_{3/2}, M_2 = \frac{g_2^2}{16\pi^2} m_{3/2}, M_3 = -3\frac{g_3^2}{16\pi^2} m_{3/2}$$

$$A_y = -\frac{\beta_y}{y} m_{3/2} \;\&\; m_\phi^2 = -\frac{1}{4}\left(\frac{\partial\gamma}{\partial g}\beta_g + \frac{\partial\gamma}{\partial y}\beta_y\right) m_{3/2}^2 + m_0^2$$

$\boldsymbol{m_{3/2}}$***, m$_0$, tan β, sign (μ)***

RGE ⇒ $M_1 : M_2 : |M_3| \approx 2.8 : 1 : 7.1$ *including 2-loop conts*

Chattopadhyay et al,PRD 07

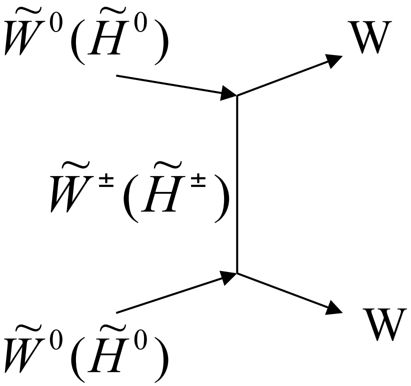

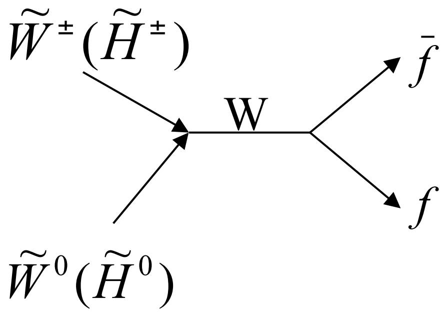

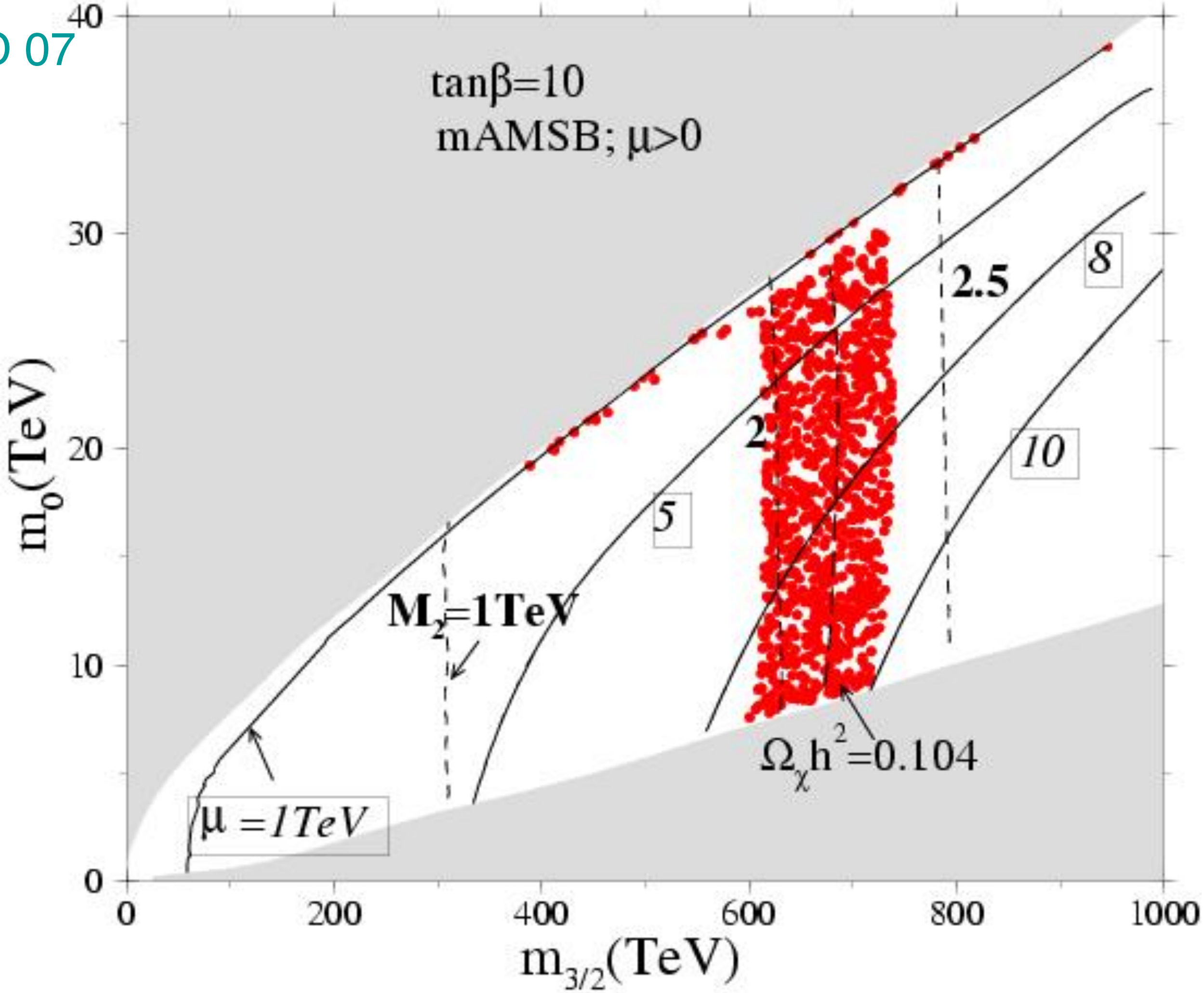

$$\widetilde{W} - LSP : M_2 = 2.1 \pm 0.2 TeV \ \& \ \widetilde{H} - LSP : \mu \cong 1 TeV (m_\phi = 10 - 30 TeV)$$

Robust results, independent of other SUSY parameters
(Valid in any SUSY model with Wino(Higgsino) LSP)

3. Detection of HE γ Rays from Galactic Centre in ACT (HESS,CANGAROO,MAGIC,VERITAS)

$$\chi \cong \tilde{H}^0 \& \tilde{W}^0, \tilde{B}^0$$

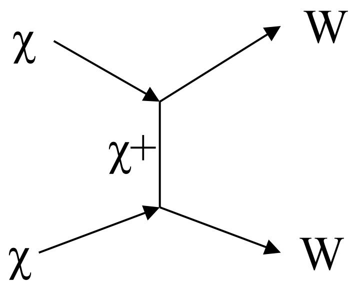

W→π^0s→γs

vσ ~ 10^{-26} cm^3/s
⇒Cont. γ Ray Signal
(But too large π^0→γ from Cosmic Rays)

$$\tilde{B}^0 - LSP \Rightarrow \chi\chi \xrightarrow{A} \bar{b}b, b \rightarrow \pi^0 s \rightarrow \gamma s$$

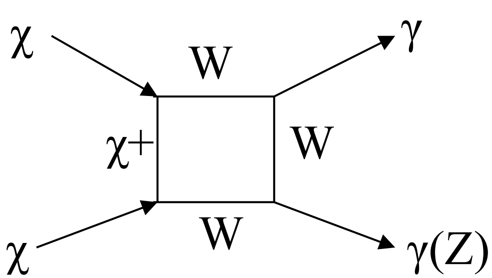

$v\sigma_{\gamma\gamma} \sim v\sigma_{\gamma Z} \sim 10^{-27}$-$10^{-28}$ cm^3/s
⇒Discrete γ Ray Line Signal ($E_\gamma \approx m_\chi$)
(Small but Clean)

Reconciling Heavy Wino DM Model with the Relic Density and PAMELA Data with Sommerfeld Enhancement:

Mohanty, Rao & Roy: IJMP A27, 1250025 (2012)

$$\chi\chi \xrightarrow{\chi^{\pm}} W^{+}W^{-}$$

Enhanced by multiple W boson exchange ladder diagram (Sommerfeld Resonace)
→ Increase of DM Annihilation CS and decrease of relic density at Resonance Peak

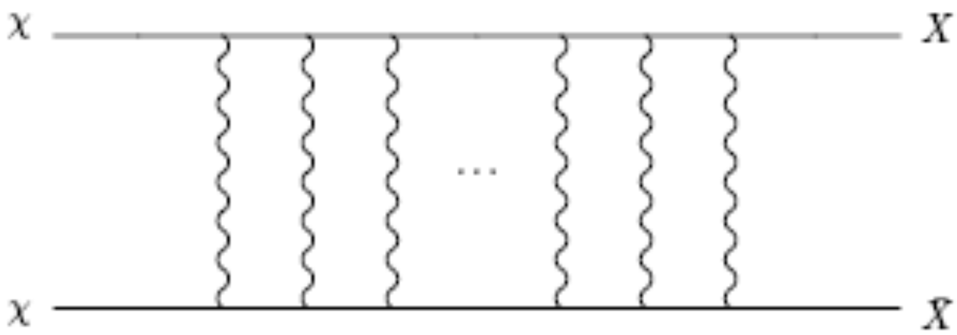

FIG. 1: Ladder diagram giving rise to the Sommerfeld enhancement for $\chi\chi \to X\overline{X}$ annihilation, via the exchange of gauge bosons.

Hisano,Matsumoto.Nojiri' 03
………………..
Lattanzi,Silk '09

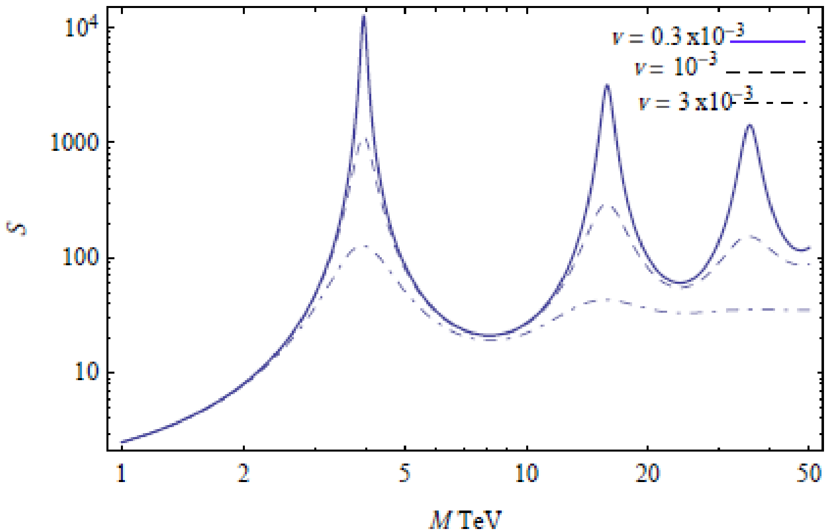

Fig. 1. Sommerfield enhancement from W exchange as a function of the DM mass for different relative velocities.

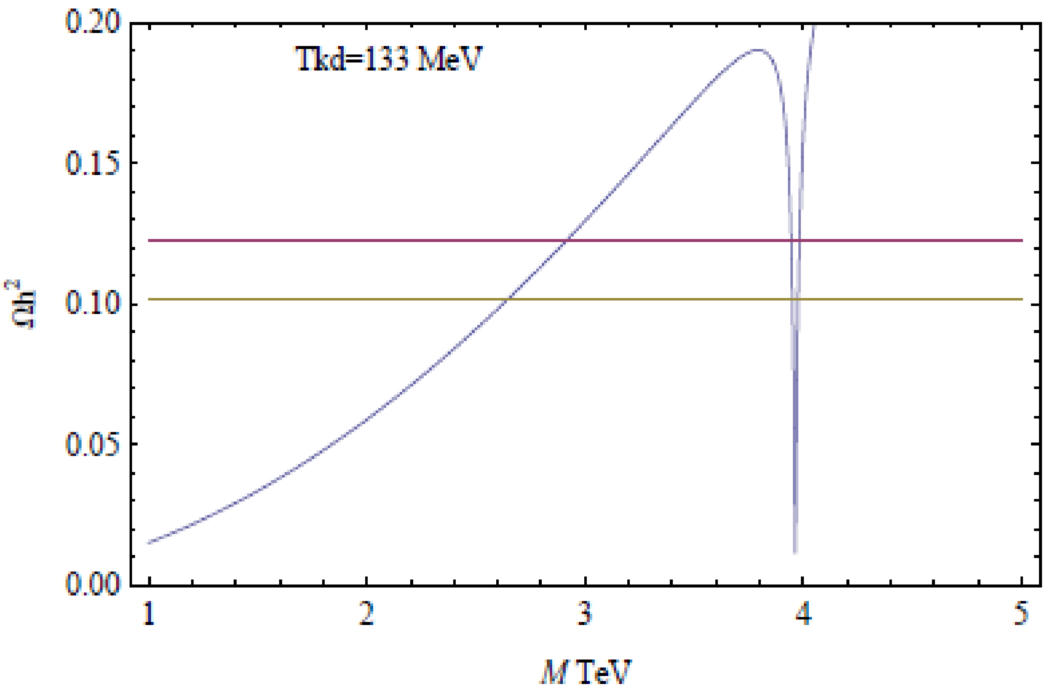

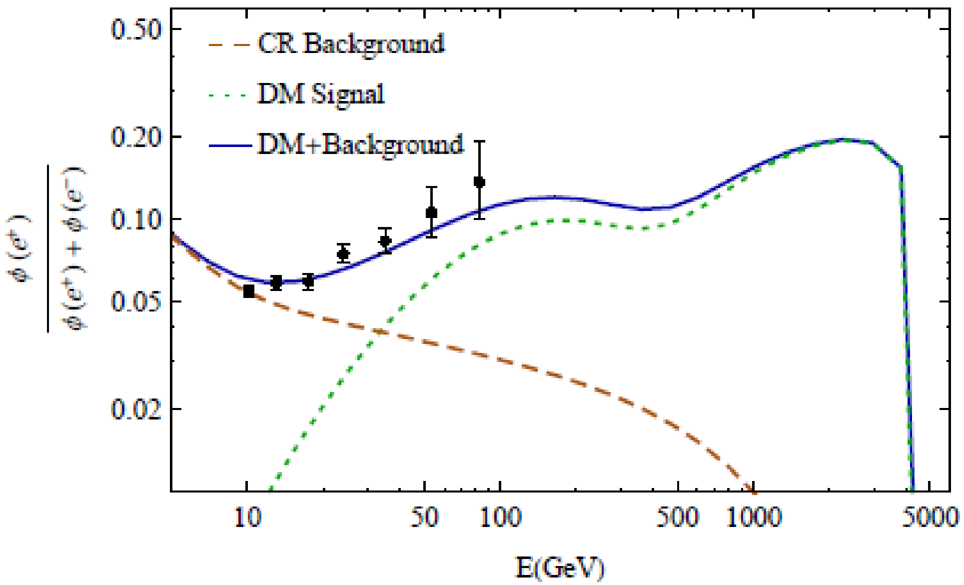

Fig. 9. Positron flux ratio for the 3.98 TeV wino DM compared with PAMELA data.[1] Dashed line shows background from cosmic ray secondary positrons.